Comparison of Various Radiation-cooled Dew Condensers by Computational Fluid Dynamic

O. Clus^{a,b}; J. Ouazzani^{b,c}; M. Muselli^{a,b*}; V. S. Nikolayev^{b,d}, G. Sharan^{b,e}, D. Beysens^{b,d,f}

^a Université de Corse, UMR CNRS 6134, Route des Sanguinaires, 20000 Ajaccio, France

^b International Organization for Dew Utilization, OPUR, 60, rue Emeriau, 75015 Paris, France

^c Arcofluid SARL, Parc Unitec 1, allée du doyen G. Brus, 33600 PESSAC, France

^d Equipe du Supercritique pour l'Environnement, les Matériaux et l'Espace, PMMH/ESPCI-CNRS and

Universities Paris 6 and Paris 7, 10, rue Vauquelin, 75231 Paris, Cedex 05, France

^e Indian Institute of Management, Ahmadabad (India)

f Service des Basses Températures, CEA-Grenoble, Grenoble, France

Abstract. Radiation-cooled dew water condensers can be used to provide complementary potable water resource. In order to enhance the water yield, a Computational Fluid Dynamic (CFD) software *PHOENICS* is used to simulate several innovative condenser structures. The sky radiation is calculated for each of the geometries. Several types of condensers under typical meteorological conditions are investigated by means of their average radiating surface temperature. They are compared between them and a 1 m², 30° tilted planar condenser used as a reference. The simulations are tested against dew yield measurements. A robust correlation between the condenser cooling ability and the corresponding dew yield is found. The following shapes were studied. (1) 7.3 m² funnel shape, whose best performance is for cone half-angle of 60°: compared to the reference condenser, the cooling efficiency is improved by 40%, (2) 0.16 m² flat planar

^{*} Corresponding author, FAX: 33 4 95 52 41 42, email address: marc.muselli@univ-corse.fr

2

condenser (another dew standard), giving 35 % lower efficiency than the 30°, 1 m² reference. (3) 30 m², 30° tilted planar condenser (representing one side of a dew condensing roof), whose yield is the same as the reference. (4) 255 m² multi ridge condenser (some elements of a dew water plant), which gives results similar to the reference at windspeed below 1.5 m/s and higher yields by about 40 % at windspeed larger than 1.5 m/s.

Keywords - Dew water - Water - Computational Fluid Dynamics (CFD) - Radiative cooling

Desalination Volume 249, Issue 2, 15 December 2009, Pages 707-712

INTRODUCTION

Dew condensation obtained with radiative cooling can be an interesting complementary renewable source of potable water, especially for arid or insular areas [1-6]. Radiative cooled dew condensers are in general composed of a film (foil) including mineral particles with high IR emissivity (plastic film: produced by OPUR [2,7]; paints: [8]). This film is placed on a thermal insulation layer (polystyrene foam or Styrofoam). This foil is passively cooled below the dew point temperature by radiative energy dissipation. Various pilot systems have been tested during the last decade and it is anticipated that large working systems will begin to be installed in near future at various locations. It is then important to have efficient computational procedures to determine the expected dew water output at a given site from condensers of given geometry, size. It is also important to have procedures to determine optimal design features - size, shape, orientation of installation - given the local meteorological parameters and the desired dew water output. The procedures currently available are more effective for some shapes, less for others. For instance, the detailed description of the condenser behaviour requires the determination of the heat transfer coefficient surface/air, which can be calculated for planar surfaces with (laminar) air flow parallel to the surface [1, 9] [10]. However, a calculation of the heat exchange in more complex structures submitted to turbulent air flow is much more difficult to carry out.

Experimental outdoor tests require measuring a large number of parameters, including the meteorological parameters, to be collected on a long time (typically one year) to average the season dependence. The results obtained with one specific geometry are difficult to extrapolate to another. Computational Fluid Dynamics (CFD) can then be very useful in determining the main characteristics of future condensing structures. These simulations indeed permit to (i) understand the thermal behaviour in some limit weather conditions such as very weak and very large wind speeds; (ii) optimize the condenser shape and its

implementation in the local environment before construction; (iii) predict its behaviour when changing the scale (i.e. going from a model prototype to a large system).

PROGRAM SETUP

A simulation of the condenser heat exchange must account for the following features. (i) Thermal behaviour of the radiative material and the insulation material, including its emissivity ε , thermal conductivity k and heat capacity C. (ii) Radiative cooling power, which depends on the condenser geometry and also on atmospheric conditions (sky emissivity ε_s , air temperature T_a , cloud cover N). (iii) Incoming diffusive and convective (free or forced) heat exchange with air, which depends on wind speed V, wind speed direction and condenser geometry.

Assumptions and modelling procedures

- (i) A Cartesian coordinate frame of reference is used.
- (ii) The fluid (air) is assumed incompressible and in a steady state. The condensation process is not accounted for in the model.
- (iii) The equations of momentum, continuity and temperature are solved with the finite volume code *PHOENICS* [11]. The density variation in the body forces, responsible for the free convection, is introduced through the Boussinesq approximation. The algorithm solution of the pressure field, which is essential for the determination of the velocity field, is obtained using the SIMPLEST algorithm based on the SIMPLER algorithm coupled with PARSOL. The latter is a technique for improving the accuracy of flow simulations for situations in which a fluid/solid boundary intersects obliquely some of the cells of a Cartesian or polar co-ordinate grid.
- (iv) The solid bodies (condensers) are digitized into elementary cells (volume V_c) within a 2 cm size mesh. At the interface with the outer space around the solid bodies, a correction of flux (momentum and energy)

has to be made around the solid facets that make a non zero angle with the Cartesian frame of reference. The technique used is a triangulation derived from the well-known "cut and cell" technique [12]. At the interface between the solid body and the outer space, the mesh is made variable according to a precision criterion (relative deviation smaller than 0.1 %). Both 2D and 3D simulations can be performed. An example of objects placed in the framed space is presented in Fig. 1.

(v) Boundary conditions are given for velocity Cartesian components and temperature. We assume a wind profile with a logarithmic variation in the vertical direction and a fixed air temperature at the inlet of the domain. At the surfaces (ground and condensers) are applied either conditions of fixed temperature or flux type (radiative cooling). They are given for each case below.

Figure 1

Types of condensers studied

All the condensers studied are made with radiative surface material of thickness 0.2 mm or 0.3 mm exposed to the sky and insulated from below with a thermal insulation of 2.5 cm (one inch) or 3 cm thickness. There is an exception: a small horizontal plane condenser set up on an electronic balance. It is sometimes used as a reference. It is made of a 5 mm thick plate of Plexiglas (Polymethylmethacrylate, abbreviated hereafter as PMMA) thermally isolated by an aluminum foil in contact with the plate and a 5 mm thick sheet of polystyrene foam beneath the foil.

Initial conditions and other given inputs in simulations

The initial values for thermodynamic parameters are given for each cell center and cell sides. The radiative balance E_c is added as input for each radiator elementary cell and a logarithmic type wind profile $V_c(y)$

$$V_c(y) = V_{10} \ln(y/y_0) / \ln(10/y_0)$$
 (1)

is given at the inlet of the simulated space where y (m) is the height of the cell center of the inlet, V_{I0} is the wind speed at 10m height and y_0 (here = 0.1 m) is the roughness length for each numerical experiment.

Simulation results

PHOENICS gives us the full 3D fields of the three components of velocity, the pressure variation and the temperature. We obtain also the temperature at any point (cell) of condenser surface as a function of the inlet velocity values. Using the latter output, the efficiency of the condensers of different geometry and size can then be directly computed and compared.

Imposing a specific radiative cooling power to the condenser is not achievable in the program as it is a pure surface property. We thus convert the surface cooling power into a uniform volumetric heat flux using the following approach [13]. In order to have sufficient accuracy in the calculation of the heat fluxes with the cut and cell triangulation technique, the equivalent thickness of the radiative foil has to be larger than the mesh size (2 cm). We have taken the value $e_c = 4$ cm which has been imposed in all the simulations.

The following reduction laws have to be respected between each elementary units of the virtual material (properties: thickness e_c , volume heat capacity C_c , thermal conductivity k_c) and the corresponding unit of the real material (properties: thickness e_M , volume heat capacity C_M , thermal conductivity k_M).

Conservation of heat capacity per unit surface:

$$C_{M}e_{M} = C_{c}e_{c} . (2)$$

Conservation of the heat flux component perpendicular to the material

$$\frac{k_M}{e_M} = \frac{k_c}{e_c} \quad . \tag{3}$$

This equation is reminiscent of the Newton's law of cooling [13]. The correction for the thermal conductivity is isotropic and thus increases the heat flux components parallel to the condenser surface. The consequence of this is an artificial homogenisation of the temperature in volume of the condensing

material. In this work where it is only question of studying the differences between the condenser surface temperature with the ambient air temperature, we will limit the study to only the surface temperatures.

The condensed water mass is not calculated, which corresponds to study the radiator in a dry atmosphere. However, this surface temperature is a good indicator of the condenser efficiency as shown in the following.

Radiative cooling

What matters in radiative cooling – and then in dew formation – is the difference between the condenser outcoming radiative power P_r and the sky incoming radiative power P_s . The local radiative power, P_s emitted by a source depends on the local temperature T through the Stephan-Boltzmann law,

$$P = \varepsilon \, \sigma (T + 273)^4 \,, \tag{4}$$

where σ is the Stephan-Boltzmann constant and ε is the emissivity of the surface. When considering a more complicated surface, such as the cone in Fig.1, one has to evaluate the radiation power emitted by each surface element over a given sky solid angle element and integrate over the total condenser structure and visible sky solid angle. This necessitates considering both the surface directional emissivity (that varies as the cosine of the angle with the normal to the surface element) and the sky directional emissivity $\varepsilon_{s,\theta}$. We use an approach and a formulation [14] where the sky emissivity is given by:

$$\varepsilon_{s,\theta} = 1 - \left(1 - \varepsilon_s\right)^{1/b \cos \theta} . \tag{5}$$

Here θ is the angle inclination with vertical (as in Fig.1), b = 1.66 and ε_s is the total sky emissivity, which depends on RH. For average conditions $RH \approx 80\%$, $\varepsilon_s \approx 0.8$ [1]. (Due to this specific θ dependence, the lowest atmospheric layer contained in the first 15° solid angle emits a significant amount (25%) of the total IR sky radiation.) The radiative budget is then integrated over the radiator surface and the open sky (see the funnel example in Fig. 2) by using a specific integration program.

All calculations have been carried out with a condenser taken as a "grey" body with emissivity $\varepsilon_c = 0.94$ [9] and a sky radiation corresponding to common night weather conditions in a temperate climate (e.g. Europe): clear sky, $T_a = 288$ K (15°C) ambient temperature, RH = 85% relative humidity, corresponding to the dew point temperature $T_d = 12.5$ °C. The integrations of the radiative budget are computed for various radiator temperatures T_c (from 255 K to 315 K by step of 1 K). Then a third degree polynomial law correlates the radiative budget with T_c . Eventually, each cell (temperature T_c) is programmed for dissipating an energy that depends on T_c and the cell volume.

RESULTS

Funnel shape simulation

A priori, the funnel shape should reduce the heat exchange of the condenser surface with the flow of warmer air. It also reduces the free convection along the surface by blocking the heavier cold air at the bottom. In addition, the result is independent of the wind direction because of the cone symmetry with respect to the vertical axis (y). Assuming a symmetric temperature distribution with respect to y over the internal funnel surface, all simulation cells are in radiative equilibrium with the remaining part of the surface, so that the internal radiative budget is null. In addition, in masking the lower (and most IR emissive) atmospheric layer to most of the surface, the funnel shape lowers the intensity of downward long wave sky radiation and thus enhances the radiative cooling power. Cooling is thus expected to be increased and condensation enhanced with respect to the inclined planar condenser.

An inverted pyramid with an angle $\alpha = 30^{\circ}$ with horizontal for the 4 condensation sides has already been modelled and tested [10]. A 3 cm thick Styrofoam was used as insulation layer with the OPUR foil as the

condensation surface. The area of the condensation surface was 1.11 m². The gain in dew water yield when compared with a 1 m², 30° tilted planar condenser was found close to 15%.

When dealing with a cone, choosing a smaller cone angle (larger α) reduces convection heating but also reduces radiative cooling as the radiation solid angle of the sky is lower. The goal of the simulation was to determine the optimal cone angle. For this purpose, several simulations have been tested at different wind speed and for different angles while keeping constant the cone radius constant = 1.5 m (i.e. the condenser area projected on the ground). Figure 3 shows an experimental funnel-shaped condenser equipped with the OPUR foil (of 0.2 mm thickness and emissivity $\varepsilon_c = 0.94$, placed on Styrofoam with 3 cm thickness) and its representation in *PHOENICS*.

Figure 3

Figure 4

The mean condenser surface temperature $< T_c >$ is obtained by averaging the local surface temperature over the condenser area. From simulation at different angles $\alpha = 25^{\circ}$, 30°, 35°, 40° and 50°, the $\alpha \approx 30^{\circ}$ angle (cone angle $\approx 60^{\circ}$) appears to give the best cooling efficiency (see Fig. 4). This is especially true for wind speeds exceeding 1 m/s. For lower wind speeds, the air flow is in a complicated mixed free/forced convection regime and cooling can increase at large α for moderate wind speed (0.5 m/s) although it decreases for lower speeds (0.25 m/s).

The choice of a $\alpha = 30^{\circ}$ angle for the experimental funnel condenser in Fig. 3 was thus dictated by this study. Incidentally, this angle is as well the optimal angle for plane condensers [4]. It corresponds in addition to an angle where the gravity force that drives the condensed water flow for collection is still 50% of the vertical case.

Simulation of Condensers of other shapes

We now consider the experimental condensers (Fig. 5ABCD) that have been investigated in Ajaccio since 1999 [3, 5, 15] and a large collector ("dew plant", Fig. 5E) studied in Panhandro (NW India, [6, 16, 15]). Except case A (see below), they are all equipped with the same OPUR condensing foil (emissivity ε_c = 0.94, thickness 0.20 mm placed above Styrofoam plates, 3 cm thick for ABC) and 1 inch = 2.54 cm thick for the D case). The condenser A is made of 5 mm thick plate of PMMA (emissivity $\varepsilon_c \approx 0.94$) thermally isolated by an aluminum foil in contact with the plate and 5 mm thick sheet of polystyrene foam beneath the foil.

Figure 5

As mentioned above, the condensed water mass has not been calculated and the condensers are compared only according by their surface mean temperature, $< T_c >$. It is evident that a better cooling efficiency corresponds causes a larger condensation yield h. In Fig. 6 is shown $< T_c >$ for the structures of Fig. 3 (funnel F) and Fig. 5 A, B, C, D as calculated for the "standard" weather conditions as described earlier. The results for the condensers A, F are independent of the wind direction. The condensers B, C have been orientated so as to expose their back to the dominant nocturnal wind. For the large scale ridge condenser D, three wind directions have been simulated, perpendicularly to the heap edge and from the back of the ridge ("back" wind on Fig.5d), perpendicularly to the heap edge and in front of the ridge ("front" wind, Fig. 5d) and an intermediate case where the wind makes a 30° angle with the heap edge (wind "30°" left, Fig. 5d). A detailed report of the ridge simulation results goes beyond the scope of this work [17]; we simply report for sake of comparison the temperatures corresponding to the "30°" left wind, which is the most frequent nocturnal wind.

The cooling efficiency of the condensers are compared with that of the 1 m², 30° tilted, reference condenser B by means of a relative cooling factor or "temperature gain" Δ_T defined as [4]:

$$\Delta_T = \frac{T_{cond} - T_a}{T_{ref} - T_a} \tag{6}$$

Here $T_a = 15^{\circ}\text{C}$ and T_{ref} stands for the surface temperature of the 1 m² reference condenser B. The temperature gain (Fig. 7a) as obtained from numerical simulations can reach 50%.

A good correlation was anticipated between the cooling efficiency T_c - T_a and the dew water yield. A reduced dew yield can be defined as

$$\Delta_h = \frac{h_{cond}}{h_{ref}} \tag{7}$$

where h_{cond} and h_{ref} are the dew water yields of the condenser and the 1 m² reference condenser B, respectively. Yields are expressed in the same units (mm). Data from planar condensers A, B, C, were obtained in Ajaccio from July 09, 2003 to December 06, 2003 (45 dew events) and those from the 1 m² reference condenser B and funnel condenser were gathered in Ajaccio from May 25, 2005 to November 14, 2006 (107 dew events). They are displayed in Fig. 7b. Dew yield data were also obtained on the ridge condenser D (54 dew events) and the 1 m² plane condenser B (97 dew events) in Panhandro (Kutch area, Gujarat state, NW India) from March 22, 2006 to February 27, 2007. However, no wind measurements are available for the ridges, preventing the comparison with the other data to be made. From the simulation, the ridge condenser displays different behaviour according to a cross-over windspeed value of order 1.5 m/s. Above this threshold, the ridge design prevent further heating by the wind, in a way similar to the funnel. Below this windspeed threshold, cooling is the same as for a plane condenser, most probably because the heat transfer is there dominated by free convection, making the colder air flowing down the ridges in a way similar to a tilted plane.

As shown from the comparison between Figs. 7a and 7b, the simulated Δ_T and the experimental Δ_h are indeed very well correlated, thus validating the condenser surface temperature as the key parameter to compare different condenser designs.

Figure 7

For the standard conditions, the 0.16 m² condenser A condenses (i.e. $<T_c>< T_d = 12.5$ °C) for wind speeds below 1.5 m/s while the other planar condensers still works till wind speeds of 3 m/s. The simulation of the condenser A gives indeed less cooling than the other structures, in agreement with previous studies [4]. As a supplementary comparison, Table 1 gives for each condenser type: (i) the mean relative cooling factor $<\Delta_T>$ as obtained from Fig. 7a by averaging the data between 0 and 3 m/s and (ii) the mean relative dew yield $\overline{\Delta_h} = \frac{\sum h_{cond}}{\sum h_{Ref}}$ where each summation corresponds to the addition of data in the whole measurement period. These averages have a meaning only for condensers of type A, C, F where $<\Delta_T>$ does not vary strongly with the wind speed. It is meaningless for the ridge condenser D where a steep variation is observed around windspeed 1.5 m/s. The agreement between the cooling factors and dew water yields factors is striking. Note that the funnel shape F gives indeed a cumulated dew yield about 40% larger than the 30° tilted planar condensers over the same period.

Table 1

CONCLUSION

In quantifying the ability of radiative condensers to cool down below the surrounding air temperature in presence of wind, Computational Fluid Dynamics proves to be a very powerful tool to characterize and

compare new designs for dew condensers in their precise environment. One can cite two examples: the determination of the best angle for a hollow funnel condenser - leading to a 40 % improvement with respect to an equivalent planar structure - and the determination of the best orientation of complex structures with respect to the dominant nocturnal wind. The construction of a dew plant in Panandhro (India) is one of such applications. These examples highlight the possibilities of Computational Fluid Dynamics. This technique allows key parameters to be varied in a way that is extremely difficult or even impossible for time or financial reasons to carry out by using the regular experimental field techniques. The present simulation, however, does not include condensation. Although it should be desirable to include it for a finer description, the finding of a strong correlation between the cooling ability of such radiative condensers and the experimental water yield confirms that the proposed simulation is sufficient to catch the main features of the phenomenon.

ACKNOWLEDGMENTS

This work was partly supported by the National Agency for Innovation ANVAR - OSEO - Corse. One of us (OC) was financially supported by the Collectivité Territoriale de Corse (CTC). We thank Mr. Shashank Singh who supervised the data collection in Panhandro (India).

References

- [1]. V.Nikolayev, D.Beysens, A.Gioda, I.Milimouk, E.Katiushin, JP.Morel. J. Hydrology (1996) 182:19-35
- [2]. T.Nilsson. Solar Energy Materials and Solar Cells (1996) 40:23-32
- [3]. M.Muselli, D.Beysens, J.Marcillat, I.Milimouk, T.Nilsson, A.Louche. Atmospheric Research (2002) 64:297-312
- [4]. D.Beysens, I.Milimouk, V.Nikolayev, M.Muselli, J.Marcillat. Journal of Hydrology (2003) 276:1-11
- [5]. D.Beysens, M.Muselli, V.Nikolayev, R.Narhe, I.Milimouk. Atmospheric Research (2005) 73(1-2):1-22
- [6]. G.Sharan. Dew Harvest To Supplement Drinking Water Sources in Arid Coastal Belt of Kutch. Centre for Environmental Education (Environment and Development Series, New Delhi: Foundation Books), 2006
- [7]. International Organization for Dew Utilization OPUR www.opur.u-bordeaux.fr
- [8]. M.Muselli, O.Clus, D.Beysens. Des matériaux radiatifs collecteurs de rosée. Info Chimie Magazine (2007) 482:60

- [9]. VS.Nikolayev, D.Beysens, M.Muselli. A computer model for assessing dew/frost surface deposition. Proceedings of the Second International Conference on Fog and Fog Collection 2001, St John's (Canada) July 2001 Eds.R.S. Shemenauer and H. Puxbaum, IRDC:333 336
- [10]. AFG.Jacobs, BG.Heusinkveld, S.Berkowicz. Dew and Fog Collection in a Grassland Area, The Netherlands. Proceedings of the Third International Conference on Fog, Fog Collection and Dew 2004, Cape Town, South Africa.
- [11]. DB.Spalding. Mathematics and Computers in simulation (1981) 23: 267-276
- [12]. PG.Tucker, Z.Pan. Applied Mathematical Modelling (2000) 24: 591-606
- [13]. RB.Bird, Stewart WE, Lightfoot EN. Transport phenomena (Wiley, New York, 1960) pp. 267, 283-287.
- [14]. X.Berger, J.Bathiebo. Renewable Energy (2003) 28(12):1925-1933.
- [15]. M.Muselli, D.Beysens, I.Milimouk, J. of Arid Environments (2006) 64:54-76
- [16]. G.Sharan, D.Beysens, I.Milimouk. Journal of Arid Environments (2007) 69:259-269.
- [17]. O.Clus, G.Sharan, S.Singh, M.Muselli, D.Beysens. Simulating and testing a very large dew and rain harvester in Panandhro (NW India). Proceedings of the 4th International Conference on Fog, Fog Collection and Dew, La Serena, Chile, 2007.

Figures Captions

Fig. 1. Example of a simulation grid (3 ridge condenser of Figs. 5D,d).

Fig. 2. Integration scheme for the funnel shape ($0 < \theta < \theta_L$, $0 < \varphi < 360^\circ$ and 0 < r < R).

Fig. 3. (a) Photo of the funnel-shaped condenser (7.32 m² surface area with 60° cone angle, labeled F) and (b) its 2D representation in the simulation. The internal surface of the experimental condenser is coated with OPUR Low Density PolyEthylene film insulated from below with 3 cm Styrofoam.

Fig. 4. Funnel mean surface temperature $< T_c >$ with respect to the angle α with horizontal (90° - half cone angle) at various wind speed. The angle $\alpha \approx 30^\circ$ gives the best cooling efficiency (vertical line).

Fig. 5. Real condensers (A-D) and their simulation models (a-d). The corresponding figures for the funnel condenser (labeled F) are described in Fig. 3. (a) 0.4 x 0.4 m² isolated foil on a table. (b) 30° tilted with horizontal 1 x1 m² condenser, (c) 30° tilted with horizontal 3 x 10 m² condenser. (d) Three trapezoidal ridges (top 50 cm, base 2 m, two sides 30° tilted, height 50 cm, length 34 m on a 15° slope from horizontal) in Gujarat state (NW India).

Fig. 6. Averaged surface temperatures obtained by numerical simulation and related to wind speed at 10 m elevation. No condensation occurs below the broken line $\langle T_c \rangle \langle T_d = 12.5 \, ^{\circ}\text{C}$, corresponding to $T_a = 15^{\circ}$ and $RH = 80 \, \%$.

Fig. 7. (a), "Temperature gain" (called also cooling factor) Δ_T as obtained by numerical simulations for four condensers (A-D from Fig. 5 and F from Fig. 3) with surface area ranging from 0.16 to 255 m² (T_a =

15°C and RH = 80%). The 1 m², 30° inclined planar condenser is taken as a reference. (b), "Dew gain" (called also relative dew yield) Δ_h for three types of condensers (non available for the 255 m² condenser). Data are smoothened by a 70% weighing function.

Table Caption

Table 1. Average values of relative cooling and relative yield factors for planar and funnel condensers (see text).

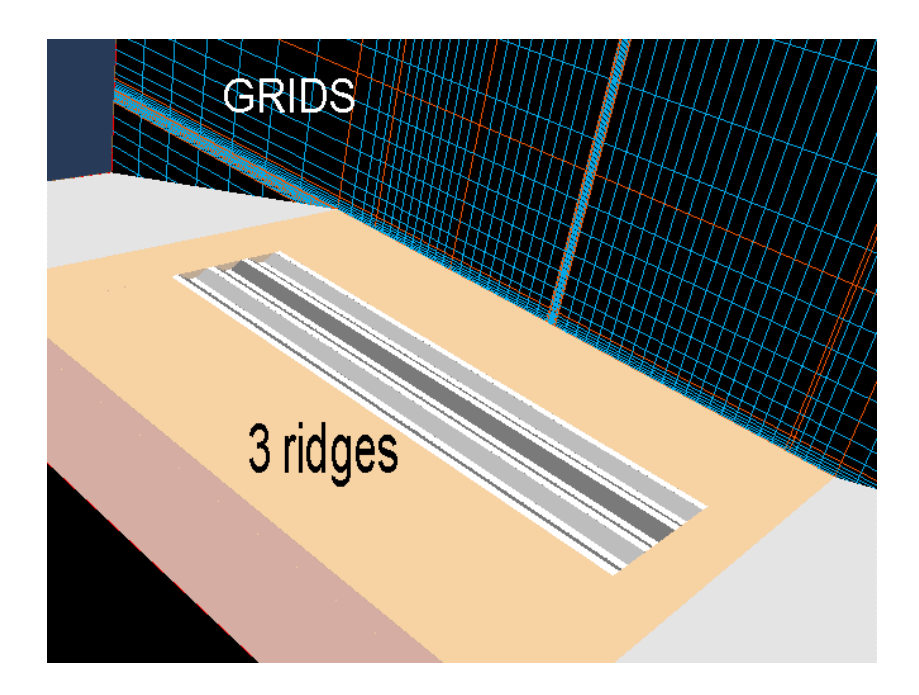


Fig. 1. Example of a simulation grid mesh (3 ridge condenser of Figs. 5D,d).

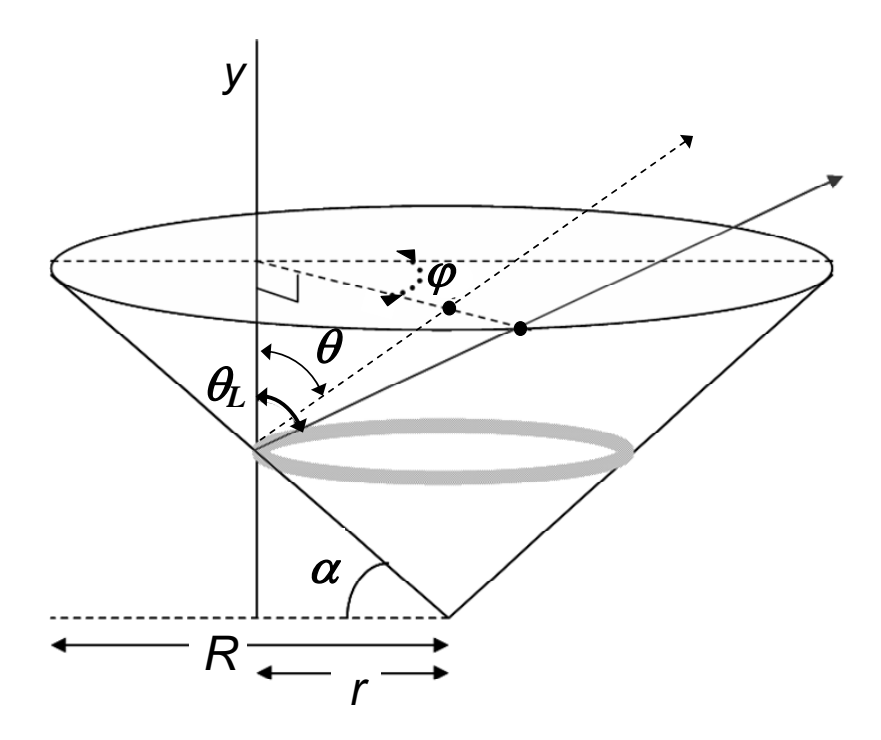


Fig. 2. Integration scheme for a funnel shape ($0 < \theta < \theta_L$, $0 < \varphi < 360^\circ$ and 0 < r < R).

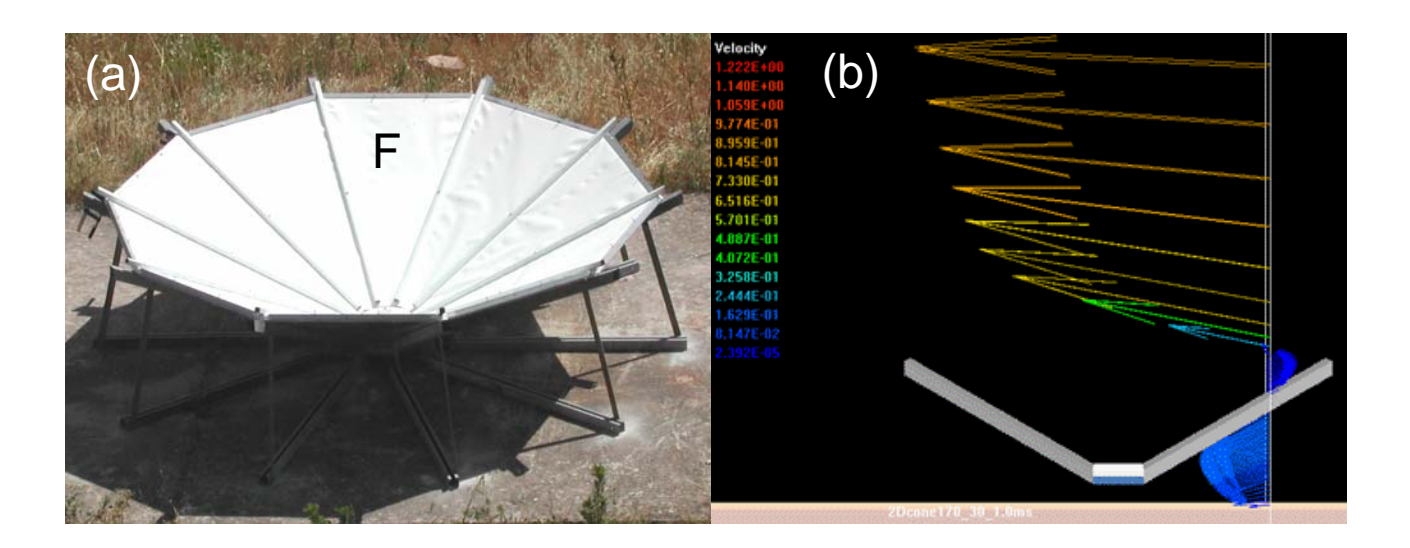


Fig. 3. (a) Photo of the funnel-shaped condenser (7.32 m² surface area with 60° cone angle, labeled F) and (b) its 2D radial representation in the simulation. The internal surface of the experimental condenser is coated with OPUR Low Density PolyEthylene film insulated from below with 3 cm Styrofoam.

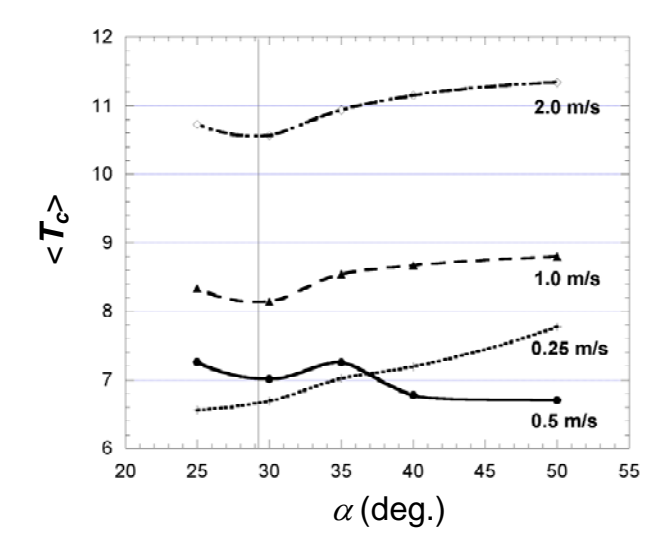


Fig. 4. Funnel mean surface temperature $< T_c >$ with respect to the angle α with horizontal (90° - cone angle θ_L) at various wind speed. The angle $\alpha \approx 30^\circ$ gives the best cooling efficiency (vertical line).

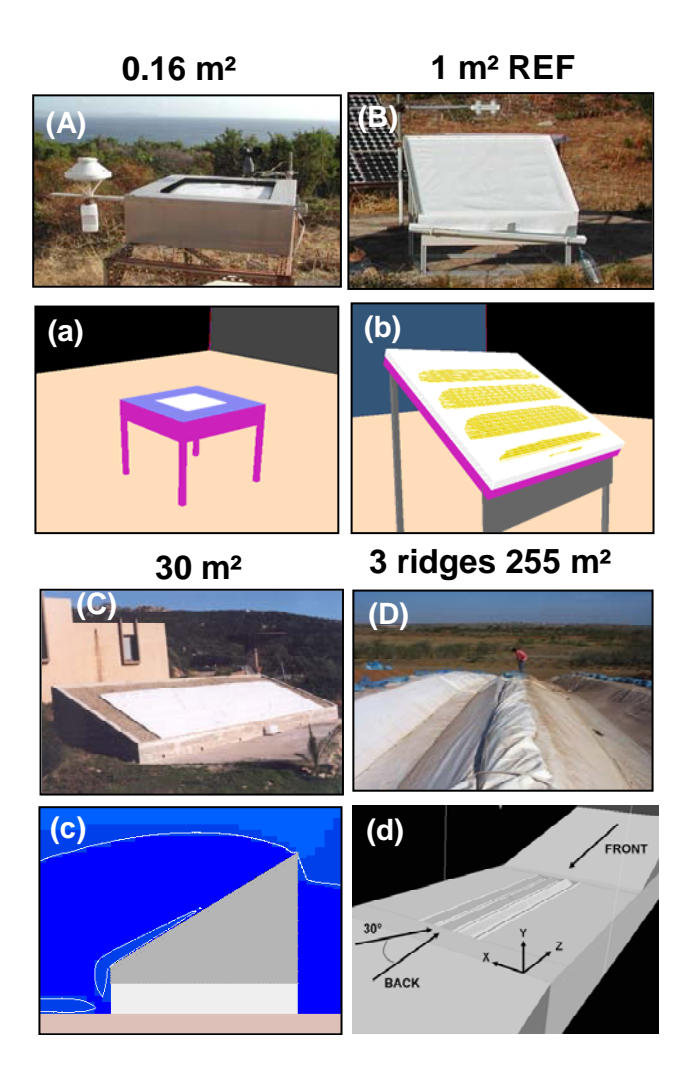


Fig. 5. Real condensers (A-D) and their models (a-d). The corresponding figures for the funnel condenser (labeled F) are described in Fig. 3. (a) 0.4 x 0.4 m² isolated foil on a table. (b) 30° tilted with horizontal 1 x1 m² condenser, (c) 30° tilted with horizontal 3 x 10 m² condenser. (d) Three trapezoidal ridges (top 50 cm, base 2 m, two sides 30° tilted, height 50 cm, length 34 m on a 15° slope from horizontal), in Gujarat state (NW India)

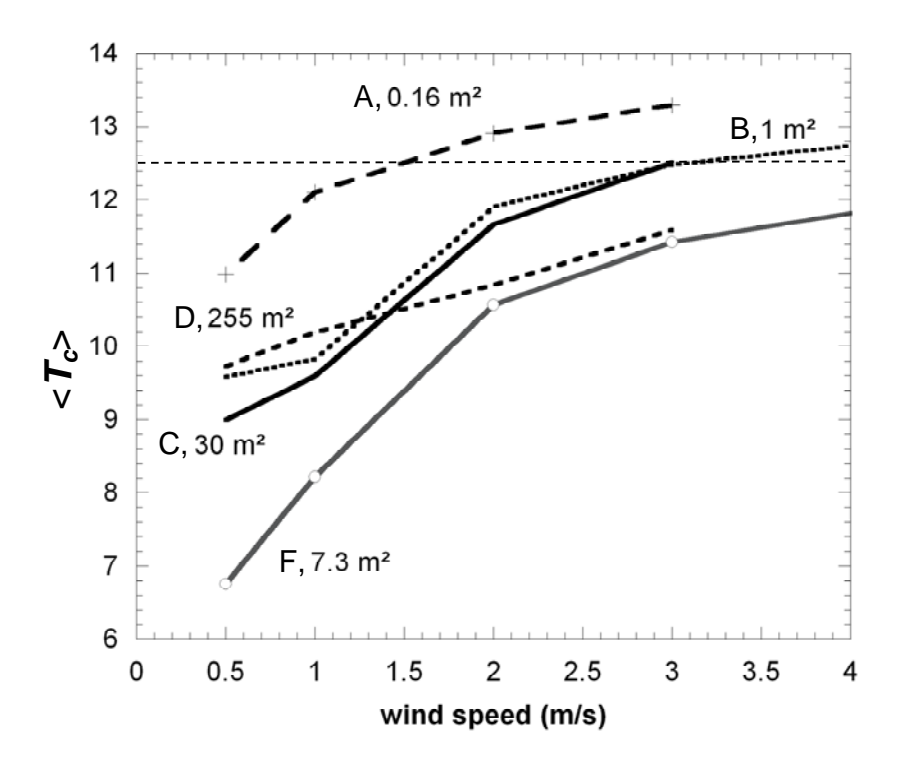


Fig. 6. Averaged surface temperatures obtained by numerical simulations and related to wind speed at 10 m elevation. No condensation occurs below the interrupted line $\langle T_c \rangle \langle T_d = 12.5$ °C, corresponding to $T_a = 15$ ° and RH = 80 %.

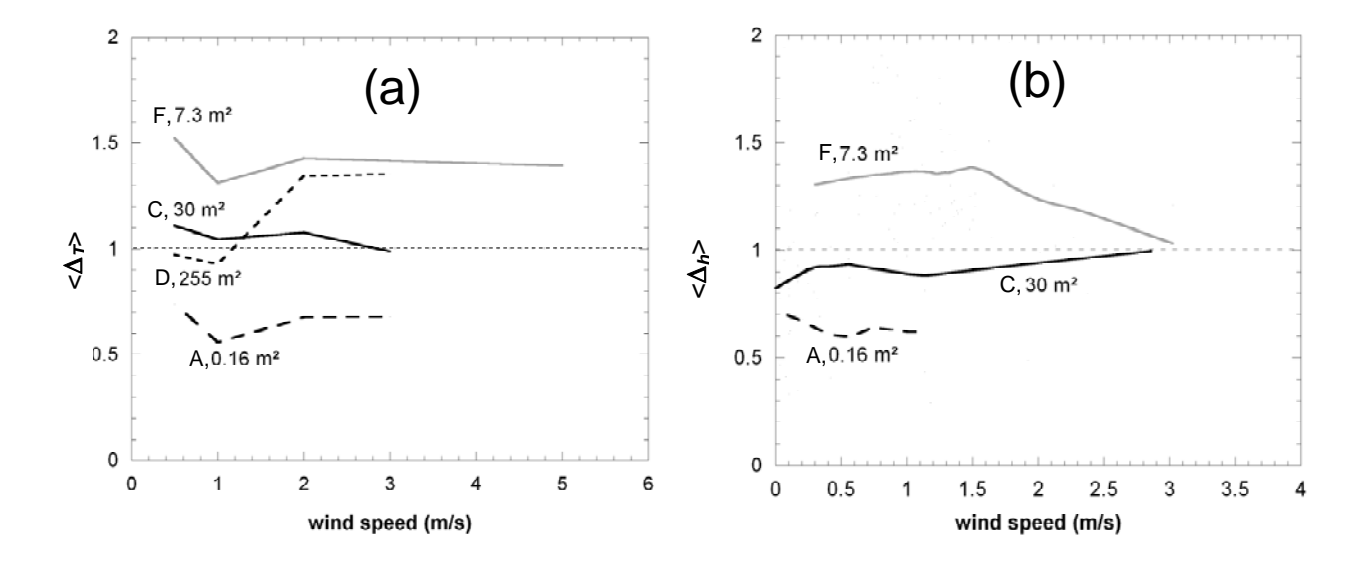


Fig. 7. (a), "Temperature gain" or cooling factor Δ_T as obtained by numerical simulations for four condensers (A-D from Fig. 5 and F from Fig. 3) with surface area ranging from 0.16 to 255 m² ($T_a = 15$ °C and RH = 80%). The 1 m², 30° planar condenser is taken as a reference. (b), "Dew gain" or relative dew yield Δ_h for three types of condensers (non available for the 255 m² condenser). Data are smoothened by a 70% weighing function.

Relative factors	A: 0.16 m^2	C: 30 m ² , 30°	F: 7.32 m ² ,
	horizontal planar	planar	funnel
Temperature $<\Delta_T>$	0.65	1.05	1.40
Dew yield $\overline{\Delta_h}$	0.68	0.91	1.38

Table 1. Average values of relative cooling and relative yield factors for planar and funnel condensers (see text).